Journal of Hazardous Materials 421 (2022) 126768

Contents lists available at ScienceDirect

Journal of Hazardous Materials

journal homepage: www.elsevier.com/locate/jhazmat

Research Paper

Plant uptake of perfluoroalkyl substances in freshwater environments (Dongzhulong and Xiaoqing Rivers, China)

Pere Colomer-Vidal [a,d], Longfei Jiang [a], Weiping Mei [c], Chunling Luo [a,c,*], Silvia Lacorte [d], Anna Rigol [b,**], Gan Zhang [a]

[a] State Key Laboratory of Organic Geochemistry, Guangzhou Institute of Geochemistry, Chinese Academy of Science, 511 Kehua Street, Wushan, Tianhe District, Guangzhou 510640, Guangdong, China
[b] Department of Chemical Engineering and Analytical Chemistry, Faculty of Chemistry, University of Barcelona, Martí i Franquès 1-11, 08028 Barcelona, Spain
[c] College of Natural Resources and Environment, South China Agricultural University, 483 Wushan Road, Tianhe District, Guangzhou 510642, China
[d] Department of Environmental Chemistry, IDAEA-CSIC, Jordi Girona 18-26, 08034 Barcelona, Spain

ARTICLE INFO

Editor: Dr. R Sara

Keywords:
PFASs
PFOA
Xiaoqing River
Water-sediment partitioning
Plant uptake

ABSTRACT

This study provides new knowledge on the mobility, behavior, and partitioning of 17 perfluoroalkyl substances (PFASs) in the water-sediment-plant system along the Dongzhulong and Xiaoqing Rivers. The fate of PFASs in these rivers is also discussed. The study area is affected by the industrial production of perfluorooctanoic acid (PFOA). The ∑PFASs in water and sediments close to the industrial discharge were 84,000 ± 2000 ng/L and 2300 ± 200 ng/g dw, respectively, with the concentrations decreasing along the river due to dilution. PFOA was the dominant compound (74–97% of the ∑PFASs), although other PFASs were identified close to urban areas. Principal component analysis and solid-liquid distribution coefficients revealed that long-chain PFASs accumulated in the sediment whereas short-chain PFASs remained in the water all along the river. PFASs were taken up by plants and remobilized to different plant compartments according to shoot concentration factors (SCFs), root concentration factors (RCF), and transfer factors (TFs). Among the four plant species studied, floating plants absorbed high levels of PFASs, while rooted species translocated short-chain PFASs from the roots to the shoots. Therefore, floating species, due to their high uptake capacity and large proliferation rate, could eventually be used for phytoremediation.

1. Introduction

Perfluoroalkyl substances (PFASs) are industrial compounds whose production started in the 1950s for commercial purposes (Renner, 2001). PFASs have excellent thermal and chemical stability and are used as polymers, surfactants, stain repellents, and flame retardants in several products such as carpets, leather, paper, textiles, and fire-fighting foams (Renner, 2006), as well as in essential products such as medical devices and occupational protective clothing (Cousins et al., 2019). PFASs are ubiquitous in the environment through their presence in discharges from various point sources such as manufacturing and processing industries, as well as in aqueous film-forming foams (Barton et al., 2020), wastewater discharges, sewage sludge (Stahl et al., 2018), landfills, and air emissions (Wang et al., 2014a). They remain in the aquatic system due to their persistent and bioaccumulative properties (Wang et al., 2014b).

Once in the environment, PFASs can remain solubilized in water, sorb into sediments, or be taken up by plants. It depends on the physicochemical properties of the compounds (e.g., perfluorocarbon chain length, head of the functional group, water solubility, and volatility), plant physiology (e.g., transpiration rate, and lipid and protein contents), and abiotic factors (e.g., soil organic matter, pH, salinity, and temperature) (Wang et al., 2020). To evaluate the accumulation and mobility of PFASs in the water-sediment-plant system, partitioning factors (K_d) (Milinovic et al., 2015) and plant uptake rates (Bizkarguenaga et al., 2016; Wang et al., 2020) are important as they provide information on the distribution and final fate of PFASs. However, these processes have not been widely studied in a river basin affected by local discharges of PFASs from a manufacturing plant and in the transport of

* Corresponding author at: State Key Laboratory of Organic Geochemistry, Guangzhou Institute of Geochemistry, Chinese Academy of Science, Guangzhou 510640, Guangdong, China.
** Corresponding author.
E-mail addresses: clluo@gig.ac.cn (C. Luo), annarigol@ub.edu (A. Rigol).

https://doi.org/10.1016/j.jhazmat.2021.126768
Received 15 March 2021; Received in revised form 1 July 2021; Accepted 26 July 2021
Available online 28 July 2021
0304-3894/© 2021 The Authors. Published by Elsevier B.V. This is an open access article under the CC BY license (http://creativecommons.org/licenses/by/4.0/).

PFASs along a river.

As a consequence of fast economic growth over the last decades, industrial development has expanded to satisfy the global needs of PFASs and related chemicals. The People's Republic of China is one of the main producers of PFASs. The fluoropolymer-producing facility located in the highly urbanized and industrialized Bohai Sea Economic Rim in northeastern China in 2012 produced 37,000 tons of polytetrafluoroethylene, 50,000 tons of tetrafluoroethylene, 10,000 tons of hexafluoropropylene, 500 tons of perfluorinated ethylene-propylene copolymers, 300 tons of polyvinylidene fluoride, 40 tons of perfluorooctanoic acid (PFOA) ammonium salt, and more than 200,000 tons of different types of fluorinated refrigerants (Wang et al., 2014b). As a result of this production, the Xiaoqing River and its Dongzhulong tributary are affected by the emissions of PFASs, with the Bohai Sea receiving around 87.3 tons per year (Chen et al., 2017) that accounts for approximately 10–30% of the global PFOA emissions (Shi et al., 2015). Due to the PFOA-manufacturing plant, this compound has been recurrently detected in water samples and sediments from the Xiaoqing River (Song et al., 2018) and the Laizhou Bay and Bohai Sea (Zhou et al., 2018; Zhu et al., 2014). However, the water-sediment partitioning factors and the role of plants in the uptake and remobilization of PFASs have not been elucidated. This information is relevant to determine the fate of PFASs in such an impacted river.

The main objective of the present study was to investigate the distribution and fate of 17 PFASs along the Dongzhulong and Xiaoqing River basin, an area receiving direct PFOA discharges from a manufacturing plant in China. Specific objectives were to: (i) evaluate the occurrence and partitioning of these 17 PFASs in surface waters and surface sediments along the river, (ii) assess the uptake of PFASs by four plant species, two floating and two rooted, and (iii) elucidate the mobilization of PFASs by plants. Principal component analysis (PCA) was used to assess the sources of pollution and distribution trends. Overall, this study provides new information on the occurrence, transport, partitioning, and plant uptake of PFASs in an impacted river to better understand the processes that explain the behavior of PFASs in real environmental conditions.

2. Materials and methods

2.1. Study area and sample collection

The study area comprised the Xiaoqing River basin. The Dongzhulong River is a tributary of the Xiaoqing River and receives industrial discharges from the biggest fluoropolymer-producing facility in China that is part of the Dongyue Group (Wang et al., 2014a–c). It also receives wastewater from major cities (Jinan, Zibo, Binzhou, and Dongying) where petrochemical, chemical, electronic, iron, and steel industries are located (Chen et al., 2017).

Eleven sampling points along the Dongzhulong and Xiaoqing Rivers were sampled in August 2017. The first sampling point was just after the water discharge area of the fluoropolymer-producing facility (0.16 km) and the last sampling point was just before a dam (38.16 km) (Fig. 1). Sampling points 1–5 were in the Dongzhulong River, while sampling points 6–11 were in the Xiaoqing River. The samples collected at each point included: (i) 1-L grab sample of surface water; (ii) freshwater surface sediment (top 0–20 cm) collected with a drag, and (iii) two plant species floating on the surface water (*Lemna minor* and *Ceratophyllum demersum*) and two plant species with roots (*Alternanthera sessilis* and *Eriochloa villosa*) collected manually alongside sediment from around the roots. For each plant species, six individuals were collected at each site and pooled, except for *L. minor* , for which a composite sample of dozens of individuals was taken due to the small individual size. Details

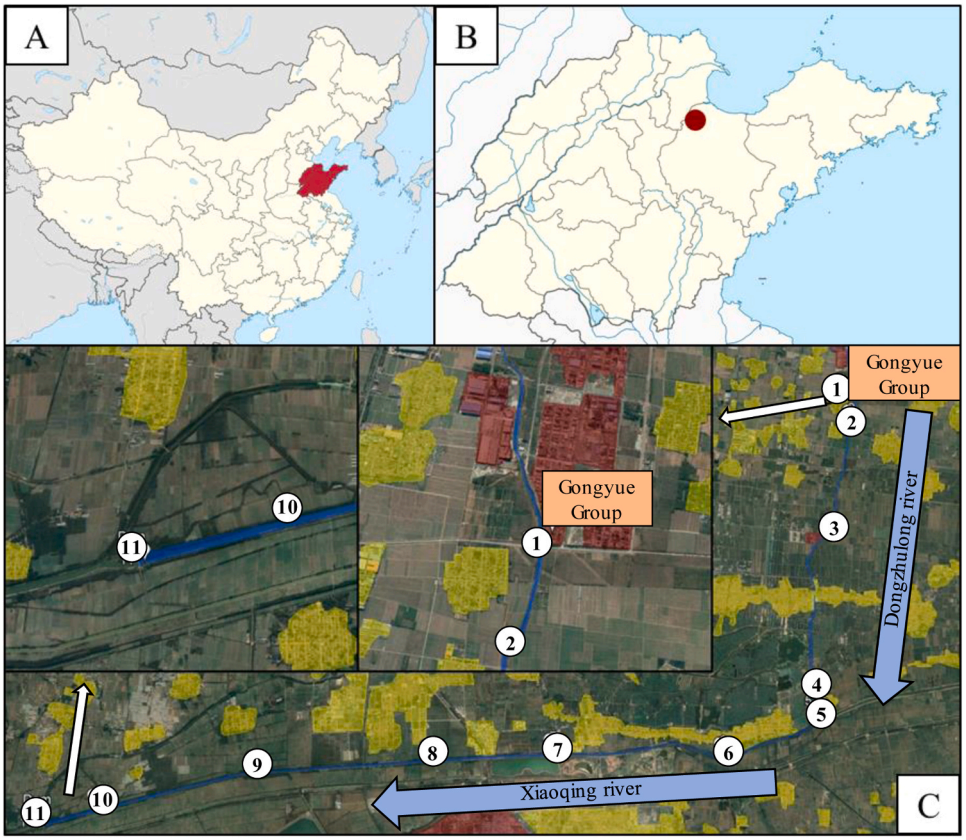

Fig. 1. Sampling area. (A) Map of China with the Shandong Province shown in red. (B) Red dot indicates the Xiaoqing River basin. (C) Map showing the river from the fluoropolymer-producing facility (red) to the dam. Urban settlements are shown in yellow, the river flow is indicated by the arrows (blue), and the sampling points are shown as white dot. (For interpretation of the references to colour in this figure legend, the reader is referred to the web version of this article.)

of the sampling information are listed in Table S1 and a further description of the plant species are provided in Supplement S1 of the Supplementary Information (SI). Not all the plants were growing at all the sampling points. Therefore, the plants reported at some of the sampling points indicate their specific presence in that given area.

Water samples were stored in cold conditions (4 ºC) until extraction. Surface sediments were freeze-dried for 48 h, homogenized with a blender, and frozen (–20 ºC) in bags before analysis. Rooted plants were divided into shoots and roots. Each part was washed sequentially with tap water and Milli-Q water and dried with tissue paper. All plant materials were freeze-dried for 48 h, homogenized with a blender, and frozen (–20 ºC) in bags before analysis. Sediments taken from around the roots were separated manually and processed as river sediments.

2.2. Chemicals and reagents

Standards of PFAS mixtures were purchased from Wellington Laboratories and contained perfluoro-n-butanoic acid (PFBA), perfluoro-n-pentanoic acid (PFPeA), perfluoro-n-hexanoic acid (PFHxA), perfluoro-n-heptanoic acid (PFHpA), perfluoro-n-octanoic acid (PFOA), perfluoro-n-nonanoic acid (PFNA), perfluoro-n-decanoic acid (PFDA), perfluoro-n-undecanoic acid (PFUnDA), perfluoro-n-dodecanoic acid (PFDoA), perfluoro-n-tridecanoic acid (PFTriDA), perfluoro-n-tetradecanoic acid (PFTeDA), perfluoro-n-hexadecanoic acid (PFHxDA), and perfluoro-n-octadecanoic acid (PFODA), potassium perfluoro-1-butanesulfonate (PFBS), sodium perfluoro-1-hexanesulfonate (PFHxS), sodium perfluoro-1-octanesulfonate (PFOS), and sodium perfluoro-1-decanesulfonate (PFDS). A working solution was prepared in methanol at a concentration of 0.2 μg/mL and stored at –18 ºC. Mass-labeled perfluoro-1-[$^{13}C_8$]-octane sulfonamide (M8FOSA-I, 1.2 mL × 50 μg/mL in isopropanol) from Wellington Laboratories was used as an internal standard (IS). M8FOSA-I was prepared in methanol at a concentration of 1 μg/mL and was stored at –18 ºC. Methanol and acetonitrile were supplied by Merck & Co (New Jersey, USA), tetrabutylammonium hydrogen sulfate (TBAHS) by Sigma-Aldrich (St. Louis, USA), and methyl tert-butyl ether (MTBE) by Macklin (Shanghai, China). Supelclean ENVI-Carb SPE Tube cartridges were obtained from Supelco (Bellefonte, USA).

2.3. Extraction and instrumental method

Regarding surface water samples, the extraction method used was adapted from Heydebreck et al. (2015) and applied to non-filtered water in order to quantify the total concentration of PFASs in water including the small amount sorbed to particulate matter. Briefly, 100 μL of the M8FOSA-I IS at a concentration of 1 μg/mL were added to 1 L of water and solid-phase extraction (SPE) was performed at approximately 2 mL/min using the Supelclean ENVI-Carb SPE cartridges (250 mg, volume of 3 mL, obtained from Supelco). The cartridges were conditioned with 10 mL of acetone, methanol, and methanol containing 0.25% ammonium hydroxide, respectively. After sample preconcentration, the cartridges were washed with 5 mL of Millipore water, dried using a vacuum pump, and finally eluted with 10 mL of 0.25% ammonium hydroxide in methanol. The extract was reduced under a gentle stream of nitrogen and reconstituted in 1 mL of methanol.

In the case of the sediments, 1 g of sample was spiked with 100 ng of the IS (100 μL of a solution at 1 μg/mL) and left at 4 ºC overnight. Solid-liquid extraction was performed (3 times) with 5 mL of methanol and 5 mL of dichloromethane in an ultrasonic bath for 20 min, before the mixture was centrifuged (10,000 rpm, 30 min). The resulting supernatant was collected and evaporated under a gentle stream of nitrogen. The extract was reconstituted in 9 mL of water and extracted with SPE cartridges (Supelclean ENVI-Carb SPE Tube; Supelco), which were conditioned with 4 mL of methanol and 4 mL of methanol containing 0.1% ammonium hydroxide. After the preconcentration, the sample was eluted with 4 mL of methanol and 4 mL of methanol containing 0.1% ammonium hydroxide. The extract was reduced under a gentle stream of nitrogen and filtered through a 0.22-μm nylon mesh filter and reconstituted in 1 mL of methanol.

Plant extraction was performed according to the method of Wen et al. (2013), with some modifications. Briefly, 1 g of shoot or root was spiked with 100 ng of the IS (100 μL of a solution at 1 μg/mL) and 4 mL of methanol containing 0.4 mol/L of NaOH were added and left overnight at 4 ºC. Solid-liquid extraction was conducted (3 times) with 4 mL of 0.25 mol/L of the sodium carbonate buffer, 2 mL of 0.5 mol/L of TBAHS, and 5 mL of MTBE. The mixture was manually shaken for 20 min and centrifuged (4200 rpm, 10 min). The supernatant was reduced under a gentle stream of nitrogen, filtered through a 0.22-μm nylon mesh filter into a chromatography vial, and reconstituted in 1 mL of methanol.

PFASs were analyzed using a Liquid Chromatography system from the Agilent 1220 Series coupled to an Agilent 6410 Triple Quadrupole Mass Spectrometer (Agilent Technologies, California, USA) (LC-MS/MS). A Synergi Hydro-RP 80A column (150 mm × 2 mm, 4 μm particle size) was used (Phenomenex, California, USA). 5 μL of the extract were injected. The mobile phase consisted of water (A) and methanol (B), both containing 10 mmol of ammonium acetate. The chromatographic gradient started at 30% B (condition held for 10 min), increased to 70% B over 3 min, and to 90% B over 25 min, and then increased to 100% B over 5 min, which was maintained for 15 min. The flow was set at 0.2 mL/min and the column temperature was 30ºC.

A calibration curve with six points was built over a concentration of 2, 5, 10, 25, 50, and 100 ng/mL. The PFAS calibration curve, regression coefficients, and instrumental detection limits (IDL) are shown in Table S2 of the SI. Detailed recoveries of each compound can be found in Heydebreck et al. (2015) for water and in Wen et al. (2013) for plants. Method efficiency was calculated using the recoveries of the M8FOSA-I IS (10 ng/g level), which ranged from 43% to 121% in water, 52–109% in sediment, and 70–115% in plants.

2.4. Data treatment and analysis

The pollutants partitioning between water and sediments were studied through the solid-liquid distribution coefficient (K_d, L/kg).

$$K_d = \frac{[\text{PFAS ng/kg dw}]\text{in sediment}}{[\text{PFAS ng/L}]\text{in surface water}} \quad (1)$$

The transfer of pollutants between plant compartments and the surroundings were analyzed using the shoot concentration factor from water (SCFw) in floating species, the shoot concentration factor from sediment around the root (SCFs) in rooted species, the root concentration factor (RCF), and the translocation factor (TF) between the shoot and root.

$$\text{SCFw (L/g)} = \frac{[\text{PFAS ng/g dw}]\text{in shoots}}{[\text{PFAS ng/L}]\text{in surface water}} \quad (2)$$

$$\text{SCFs (g/g)} = \frac{[\text{PFAS ng/g dw}]\text{in shoots}}{[\text{PFAS ng/g dw}]\text{in sediment around the roots}} \quad (3)$$

$$\text{RCF (g/g)} = \frac{[\text{PFAS ng/g dw}]\text{in roots}}{[\text{PFAS ng/g dw}]\text{in sediment around the roots}} \quad (4)$$

$$\text{TF (g/g)} = \frac{[\text{PFAS ng/g dw}]\text{in shoots}}{[\text{PFAS ng/g dw}]\text{in roots}} \quad (5)$$

Each quotient was calculated for the compounds detected simultaneously in the different matrices. The sediments used in the calculation of the RCF and the TF were those surrounding the roots.

PCA was performed using the R-3.4.4 software (https://www.r-project.org/). We performed PCA on PFAS concentrations detected at all the locations using the covariance matrix to explore the sources of pollution, distribution trends and patterns of association among the PFASs and the sampling points for surface water and sediments, as well

as the bioaccumulation factors (SCF and RCF) of the rooted species. We used the Kaiser–Meyer–Olkin (KMO) measure of sampling adequacy for each variable in the model and for the complete model to assess the usefulness of the PCA. The KMO value ranges from 0 to 1 and should be well above 0.5, with a value above 0.6–0.7 considered adequate for the variables to be sufficiently interdependent for PCA to be useful (Tabachnick and Fidell, 2000). In this study, the PFASs were classified by their functional group and chain length. They included perfluoroalkyl carboxylic acids with seven or fewer carbons (short-chain PFCAs), perfluoroalkyl carboxylic acids with eight or more carbons (long-chain PFCAs), perfluoroalkane sulfonates with five or fewer carbons (short-chain PFSAs), and perfluoroalkane sulfonates with six or more carbons (long-chain PFSAs) (Buck et al., 2011).

3. Results and discussion

3.1. Occurrence and partitioning of PFASs along the Xiaoqing River basin

The impact of the PFOA-manufacturing plant located at the Xiaoqing River and urban discharges of PFASs was evaluated by determining the accumulation and distribution trends of PFASs in water and sediment samples along the basin, specifically assessing the uptake ability of PFASs by different plant species. Fig. 2 shows the concentration of PFOA and ∑PFASs in water, sediment, and floating and rooted plants along the river basin. A clear dilution trend was observed from the 1st sampling point next to the fluoropolymer-producing facility to the 11th sampling point just before a dam. Consistent with the production of PFOA at the facility belonging to the Dongyue Group, PFOA was the dominant compound in all the matrices studied, comprising 74–82% of the ∑PFASs in surface water, 91–93% in sediments, and 82–97% in the floating and rooted plant species (Tables S3–S5 of the SI, respectively).

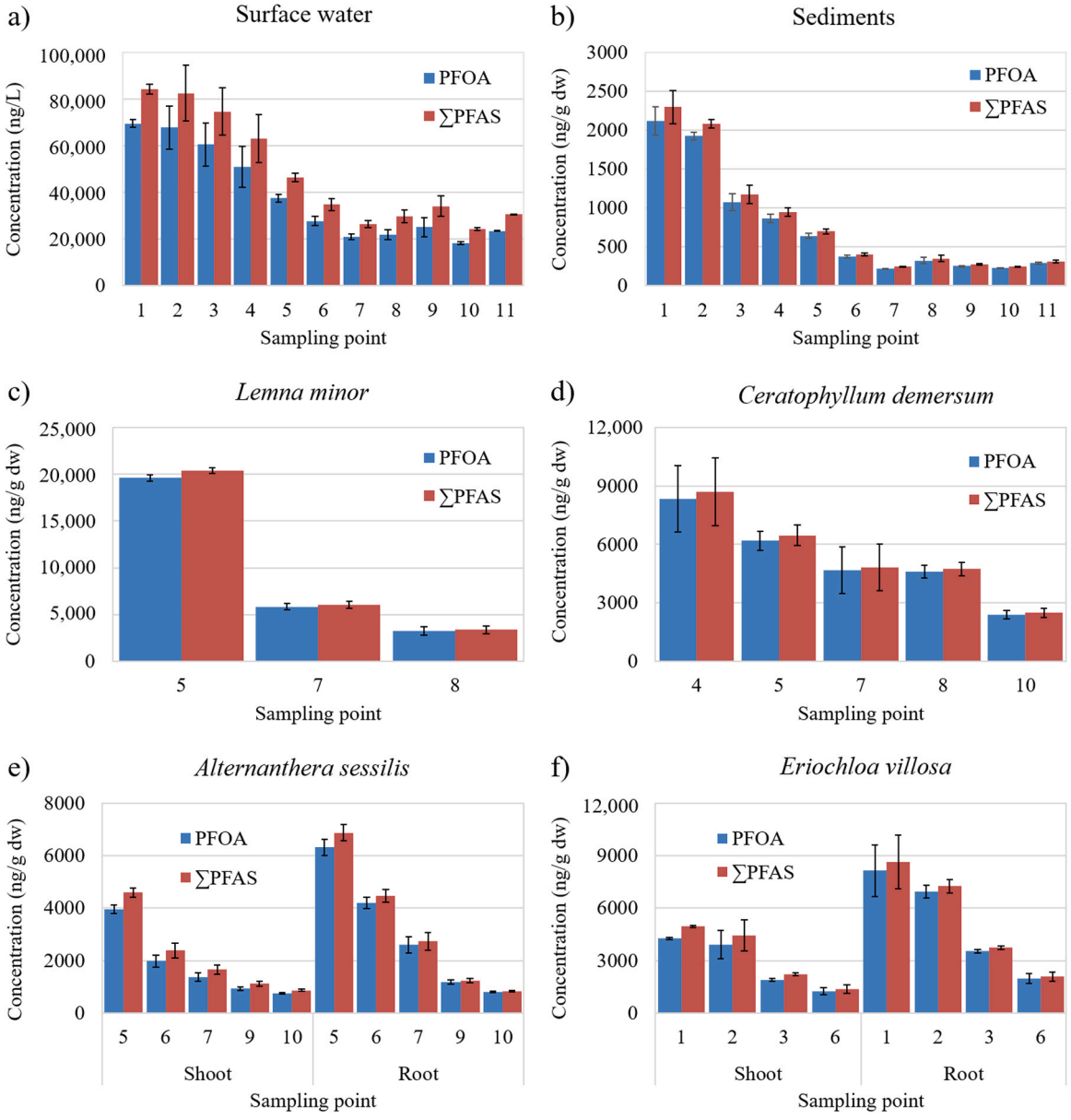

Fig. 2. Mean concentration of PFOA and ∑PFASs in (a) surface water (ng/L) and (b) sediments (ng/g dw), as well as in the shoots and roots of (c) *Lemna minor* and (d) *Ceratophyllum demersum* (ng/g dw) and in the shoots of (e) *Alternanthera sessilis* and (f) *Eriochloa villosa* (ng/g dw) at the sampling points in the Dongzhulong and Xiaoqing Rivers. Error bars indicate the standard deviation (n = 3).

3.1.1. PFASs in surface water

In surface water (Fig. 2a), PFOA had the highest concentration ranging from 18,250 ± 480 to 69,500 ± 1660 ng/L, followed by PFHxA > PFBA > PFHpA > PFPeA, which comprised 2.8–8.4% of the ∑PFASs at concentrations from 860 to 4300 ng/L (Table S6 of the SI). Long-chain PFCAs and PFSAs were found at a concentration that was one order of magnitude lower, in a range from 0.44 ± 0.04 to 374 ± 4.4 ng/L, or were not detected, as was the case for PFHxDA, PFODA, and PFDS. Our results are in agreement with those of previous studies from the Xiaoqing River that report PFOA as the dominant compound in surface water, with a concentration ranging from 4.06 to 61,900 ng/L, followed by PFHxA and PFHpA (Chen et al., 2017). Next to the same fluoropolymer-producing facility, 106,000 ng/L (Heydebreck et al., 2015) and 496,000 ng/L of ∑PFASs (Shi et al., 2015) have been recorded previously, with dilution occurring when the river waters are discharged at the Laizhou Bay in the Bohai Sea, resulting in ∑PFAS concentrations of 99.4 ng/L (Chen et al., 2016), 3.9–118 ng/L (Zhao et al., 2017), and 4.55–556 ng/L (Zhou et al., 2018). All the earlier studies report the predominance of PFOA, suggesting that the Xiaoqing River is a significant source of PFOA contamination in this area.

PCA of PFASs in surface water samples shows the distribution pattern according to scores (sample points) and loadings (compounds) (Fig. 3a). The KMO value of 0.76 indicated that the PFAS concentrations were interdependent and significantly intercorrelated with the co-predominance of all the PFASs. PCA enabled the identification of possible sources of pollution. The first and second principal components explained 69.2% and 12.5% of the total variance, respectively. PFBA, PFPeA, PFHxA, PFHpA, and PFOA had a similar contribution in the water samples, while PFNA, PFDA, PFUnA, and PFDoA were segregated, with a higher contribution at the first two sampling points. PFOS showed a high contribution at sampling point 3, located downstream of the cities of Qifengzhen, Boxing City, and Hubinzhen, with a mean concentration of 58.4 ± 13.8 ng/L. At sampling point 4, which received waters from Mata Lake (wetland and a fishing hotspot) and had irrigation channels, the mean concentration of PFOS was 93.3 ± 10 ng/L. PFOS was not manufactured nor widely applied in the industrial processes in this

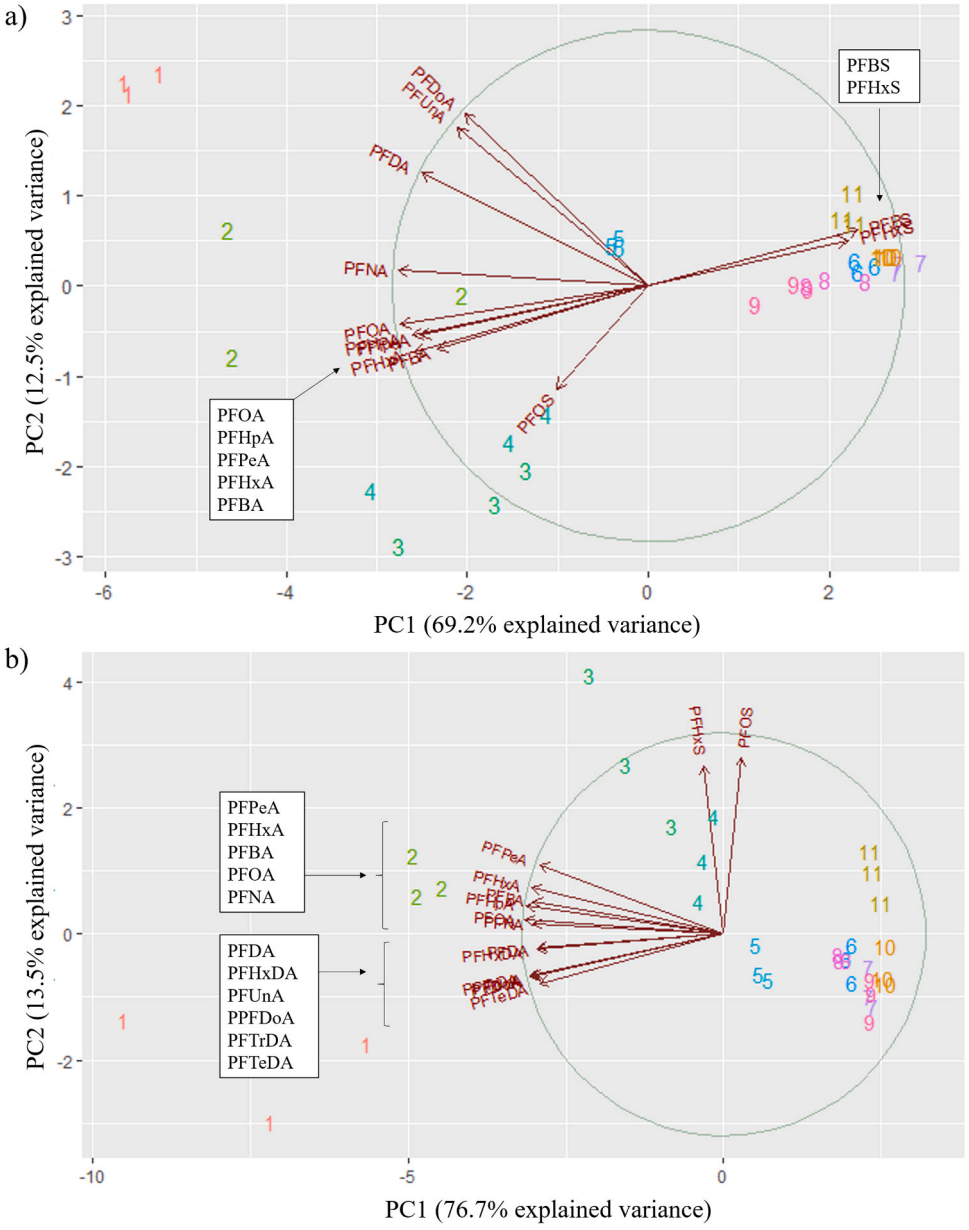

Fig. 3. PCA of the PFASs detected in (a) surface water (ng/L) and (b) sediments (ng/g dw) along the Dongzhulong and Xiaoqing Rivers. The numbers represent the sampling points analyzed in triplicate.

region (Xie et al., 2013). Previous studies have suggested that its presence is mainly from urban activities, street runoff, and wastewater treatment discharges from the very densely populated area (Shi et al., 2015). At sampling point 5, where the Dongzhulong River joins the Xiaoqing River (Fig. 1), a slight decrease in concentration was observed due to a dilution effect of both rivers, with a lower contribution in both the PC1 and PC2. Thereafter (sampling points 6–11), a specific source of PFBS and PFHxS pollution was observed in the PCA (Fig. S1 of the SI).

The high levels of PFASs found in the surface waters sampled has serious implications regarding the potential effects in wildlife as PFASs can be incorporated to organisms through diet, can be accumulated and biomagnified along the food chain and produce effects in wildlife, as observed for birds, mammals (Sonne et al., 2020), fish and other aquatic organisms (Mhadhbi et al., 2012). In addition, humans might be exposed to PFASs through the consumption of contaminated fish or edible plants and this can have effects as PFASs are cytotoxic and endocrine disruptors (Gorrochategui et al., 2016).

3.1.2. PFASs in sediments

In the sediments, PFOA was the dominant compound with a concentration of 2120 ± 182 ng/g dw at sampling point 1 and a concentration of 290 ± 17 ng/g dw at sampling point 11, thus showing a clear dilution along the basin (Fig. 2b). Previous studies in the area have reported a PFOA concentration of 3640 ng/g dw in the Dongzhulong tributary and 382 ng/g dw downstream (Shi et al., 2015). The prevalence of PFOA in sediments and the dilution effect along the Xiaoqing River basin is in agreement with previous studies reporting decreasing concentrations at downstream waters of the Xiaoqing River close to the river mouth, with Zhao et al. (2013) reporting a decreasing trend with 76.9, 2.6, and 2.1 ng/g dw and Zhu et al. (2014) reporting similar trends with 29.0, 13.0, and 2.45 ng/g dw. In terms of concentration, other PFASs were detected at levels up to 37.8 ± 8.1 ng/g dw, representing <2.4% of the ∑PFASs. PFODA, PFDS, and PFBS were not detected (Table S7 of the SI). Long-chain PFASs contributed more to the total ΣPFASs in sediment than in water due to their affinity for sediments (Chen et al., 2017; Shi et al., 2015). The PCA shown in Fig. 3b indicates that most of the PFAS concentrations were interdependent and significantly intercorrelated (KMO = 0.79). The first and second principal components explained 76.7% and 13.5% of the total variance, respectively. The first principal component was predominantly explained by PFCAs that had high concentrations at sampling points 1 and 2, while the second principal component was mainly explained by the presence of PFHxS and PFOS at sampling points 3 and 4, similar to that observed in water. PCA also showed that at sampling points 5–11, the contribution of all the PFASs was very low. For all the compounds, a decreasing trend was observed along the river, except for PFOS, whose concentration increased from sampling point 5–11, presumably due to urban effluent discharges, as observed for the water samples (Fig. S2 of the SI).

3.1.3. PFASs in plant species

There is little information regarding the accumulation of PFASs in aquatic plants, especially in real environmental conditions. The two free-floating species were the macrophyte *Lemna minor*, with a single 2-cm root, and *Ceratophyllum demersum,* a submerged, aquatic plant. The rooted species were *Alternanthera sessilis*, which has a taproot, and *Eriochloa villosa*, which has an adventitious root that branches as a taproot. Roots are known to play a major role in nutrient uptake as well as in the uptake of contaminants, thus having ecological relevance in freshwater ecosystems (Ghisi et al., 2019). The uptake of PFASs should first occur in the root of all four plant species, being absorbed either from the water or sediment (Pi et al., 2017). Fig. 2 (c–f) shows that the levels and distribution trends of PFASs in plants along the river followed that of the water and sediment samples, indicating that plants are also affected by river pollution. Throughout the river, PFOA was the main PFAS detected in all the plant species followed by short-chain PFASs. This reflects once more that the PFOA discharge area has an impact all along the river ecosystem.

In floating species, PFOA had the highest concentration, ranging from 3240 ± 430 to 19,600 ± 330 ng/g dw in *L. minor* and from 2390 ± 230 to 6190 ± 500 ng/g dw in *C. demersum*, followed by short-chain PFCAs, which had levels up to 280 ± 10 ng/g dw with a very low contribution to the ∑PFASs (Table S8 of the SI). Other PFASs were detected at lower concentrations or not detected, as was the case for PFHxDA, PFODA, PFBS, PFHxS, and PFDS. There are only a few studies on PFASs in floating plant species in the literature. ∑PFAS levels of 405 ng/g dw have been reported in *L. minor* from the Mississippi River (USA) (Oliaei et al., 2013), while levels ranging from 4.78 to 7.63 ng/g dw have been observed in *C. demersum* pooled with other aquatic plants (*Myriophyllum spicatum* and *Vallisneria spiralis*) from the Rhone River (France) (Babut et al., 2017). These levels are much lower compared to those in our study (∑PFAS levels ranging from 2500 ± 240 to 8700 ± 1750 ng/g dw).

In rooted species, the PFOA concentration in *A. sessilis* ranged from 570 ± 21 to 3960 ± 160 ng/g dw in the shoots and from 800 ± 28 to 6320 ± 310 ng/g dw in the roots. In *E. villosa*, these values ranged from 740 ± 53 to 4260 ± 42 ng/g dw in the shoots and from 1980 ± 290 to 8140 ± 1470 ng/g dw in the roots. The relatively higher levels in *E. villosa* compared to *A. sessilis* may reflect a higher root uptake due to the adventitious root of the former. However, PFHxS and PFOS had higher levels in the roots of *A. sessilis*. Tables S9 and S10 of the SI show the concentration of PFASs in the plants. Short-chain PFCAs were detected at much lower concentrations in both species, with levels up to 333 ± 35 and 126 ± 21 ng/g dw in the shoots and roots, respectively, comprising < 11% of the ∑PFASs (Tables S5, S9 and S10 of the SI). PFODA, PFBS, and PFDS were not detected. In both rooted species, most PFASs showed a general decreasing trend along the river (Figs. S3 and S4 of the SI), except for PFDA, PFUnA, PFDoA, and PFTrDA in *A. sessilis* and the shoots of *E. villosa* and PFHxS and PFOS in *E. villosa* due to their low concentrations.

3.2. Distribution of PFASs in the water-sediment system

PFASs in surface water and freshwater sediments had a similar profile along the Dongzhulong and Xiaoqing Rivers. Solid-liquid distribution coefficients (K_d) were calculated for each PFAS to assess the relationship between the chain length of the PFASs and their distribution in the water-sediment system. As illustrated in Fig. 4, the K_d values increased with the increasing chain length of the PFASs. Thus, short-chain PFCAs had low K_d values (less than 10 L/kg), indicating that these compounds are preferentially partitioned into the water as they have higher water solubility and mobility. By contrast, long-chain PFCAs, due to their higher hydrophobicity, are expected to be sorbed more readily into the organic matter in the sediment. Thus, PFOA and PFNA showed intermediate values (from 5.6 ± 0.2 to 30.5 ± 3 L/kg), while the PFASs with C-F chain >10 (PFDA, PFUnA, and PFDoA)

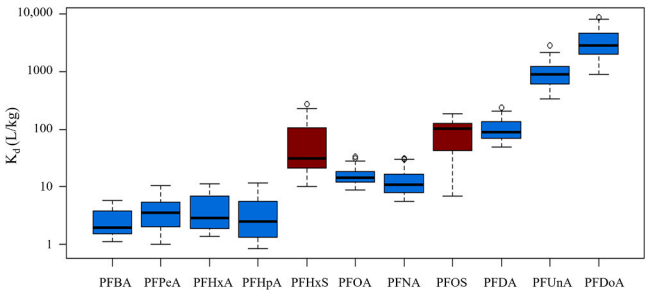

Fig. 4. Boxplot with the partition coefficient (K_d, in L/kg) in the log-10 scale for PFCAs (in blue) and PFSAs (in red), considering the different sampling points in the Dongzhulong and Xiaoqing Rivers. (For interpretation of the references to colour in this figure legend, the reader is referred to the web version of this article.)

presented the highest K_d values (from 51.8 ± 5.1 to 7800 ± 1260 L/kg), thereby preferentially accumulating in sediments. Table S11 in the SI shows the individual mean K_d values of the PFASs at each sampling point. Our results are supported by those of previous studies demonstrating that the K_d values for PFASs increase with the chain length (Liu et al., 2019a; Zhang et al., 2012). On the other hand, PFHxS and PFOS had higher K_d values than the PFCAs with the same number of fluorinated carbons (i.e., PFHpA and PFNA, respectively), suggesting that the functional group also plays a role in the distribution of PFASs in the water-sediment system. The partitioning of PFSAs into sediments is favored compared to their PFCA analogs due to their greater hydrophobicity and the larger size of the sulfonate moiety that has more specific electrostatic interactions with sediments compared to the carboxylate moiety (Higgins and Luthy, 2006).

3.3. Uptake of PFASs in floating and rooted plants

In this study, the PFAS uptake ability of floating *vs.* rooted plant species was compared and the uptake trends along the basin were evaluated. To do so, the SCFw, SCFs, RCF, and TF were calculated to assess the mobility of PFASs in the water-plant system for both floating and rooted species. Compounds not detected were omitted and were PFTrDA, PFTeDA, PFHxDA, PFODA and PFDS in water, PFHxDA, PFODA, PFBS, and PFDS in sediment, and PFHxDA, PFODA, PFBS, PFHxS, and PFDS in rooted plant species. Table 1 shows the mean values considering all sampling points. Individual values for each sampling point are indicated in Tables S12–S14 of the SI. The uptake of PFASs from water/sediment varies among plants according to the species and the environmental concentration (Krippner et al., 2014). Indeed, differences in uptake factors were observed among all four plant species in this study. PFAS concentrations in water and sediment samples decreased along the Xiaoqing River, while the PFAS profile remained constant along the sampling points. We found that floating species had a higher concentration of PFASs than rooted species at the same sampling points. Thus, uptake from water might be enhanced compared to sorption from sediments in the rooted species, with PFAS bioavailability from sediment being lower and active internal transport from the roots to shoots being required (Pi et al., 2017; Wang et al., 2020).

Regarding the floating plant species, *L. minor* and *C. demersum* had an SCFw < 1 for PFASs with 10 or fewer carbons, while SCFw > 1 for PFUnA and PFDoA, demonstrating an increase in the SCFw with an increasing chain length of the PFASs. PFOS and PFHxS also showed higher SCFw values than the PFCAs with the same chain length (PFNA and PFHpA, respectively). In concordance with our findings in floating species, a mesocosm study demonstrated that PFCAs with 10 or more carbons exhibited the highest plant-water bioaccumulation potential in *Echinodorus horemanii*, while PFASs with 4–9 carbons had the lowest bioaccumulation potential (Pi et al., 2017).

Both rooted species had a similar behavior regarding the uptake and translocation of PFASs (Fig. 5). PCA indicated that the SCFs and RCFs were interdependent and significantly intercorrelated (KMO = 0.72). The first two axes explained 51.0% and 17.5% of the total variance, respectively. Short-chain PFASs (i.e., PFBA, PFPeA, and PFHxA) positively contributed to the SCF, while long-chain PFASs (i.e., PFDA, PFUnA, PFDoA, PFTrDA, PFOS, PFOA, and PFNA) were related to the RCF. Furthermore, PFHpA had an intermediate position between these groups. We observed that short-chain PFCAs (PFBA, PFPeA, and PFHxA)

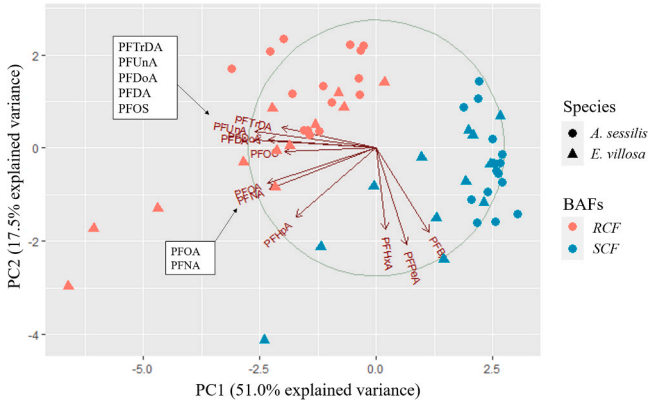

Fig. 5. PCA of the shoot concentration factor in blue (SCFs, $g_{sediment}/g_{shoot}$) and the root concentration factor in red (RCF, $g_{sediment}/g_{root}$) of PFASs in the rooted species *Alternanthera sessilis* and *Eriochloa villosa*. (For interpretation of the references to colour in this figure legend, the reader is referred to the web version of this article.)

Table 1
Mean, minimum and maximum (Mean (Min-Max)) values of the shoot concentration factor for floating species (SCFw, L_{water}/g_{shoot}), shoot concentration factor for rooted species (SCFs, $g_{sediment}/g_{shoot}$), root concentration factor (RCF, $g_{sediment}/g_{root}$), and transfer factor (TF, g_{root}/g_{shoot}) of PFASs in *Lemna minor* (n = 9), *Ceratophyllum demersum* (n = 15), *Alternanthera sessilis* (n = 15), and *Eriochloa villosa* (n = 12) collected along the Dongzhulong and Xiaoqing Rivers. Empty squares are due to the compound not being detected in the studied matrices.

	Lemna minor		*Ceratophyllum demersum*		*Alternanthera sessilis*						*Eriochloa villosa*					
	SCFw		SCFw		SCFs		RCF		TF		SCFs		RCF		TF	
	Mean (Min - Max)		Mean (Min - Max)		Mean (Min - Max)		Mean (Min - Max)		Mean (Min - Max)		Mean (Min - Max)		Mean (Min - Max)		Mean (Min - Max)	
PFBA	0.07	(0.003–0.2)	0.03	(0.01–0.06)	23	(3–39)	6	(0.5–21)	12	(1–39)	16	(7–32)	7	(3–14)	2.5	(2–3)
PFPeA	0.03	(0.008–0.08)	0.01	(0.006–0.02)	7	(3–11)	2	(0.9–4)	5	(1–10)	7	(3–19)	3	(0.5–9)	4	(1–6)
PFHxA	0.02	(0.005–0.04)	0.01	(0.005–0.02)	3	(2–5)	2	(0.6–3)	2	(1–3)	7	(3–13)	4	(1–7)	2	(1–4)
PFHpA	0.04	(0.02–0.08)	0.02	(0.01–0.03)	4	(2–6)	4	(2–8)	1	(0.5–2)	4	(2–7)	7	(3–11)	0.6	(0.4–0.8)
PFOA	0.3	(0.1–0.6)	0.2	(0.1–0.3)	2.3	(1.7–2.7)	3	(2–5)	0.7	(0.5–1)	3	(2–5)	5	(3–8)	0.6	(0.4–0.9)
PFNA	0.1	(0.02–0.2)	0.1	(0.06–0.2)	0.7	(0.3–1)	2	(1–3)	0.4	(0.2–0.6)	2	(0.6–7)	4	(2–8)	0.4	(0.2–0.7)
PFDA	0.7	(0.4–1)	0.6	(0.3–1)	0.6	(0.3–0.8)	2	(1–3)	0.3	(0.2–0.4)	0.9	(0.3–2)	3	(1–6)	0.3	(0.1–0.5)
PFUnA	4	(2–6)	3	(1–5)	0.5	(0.2–0.8)	2	(1–3)	0.2	(0.1–0.3)	0.9	(0.2–3)	2	(1–4)	0.3	(0.1–0.7)
PFDoA	11	(8–16)	7	(3–12)	0.3	(0.1–0.4)	2	(1–2)	0.2	(0.2–0.4)	0.8	(0.1–2)	2	(0.9–3)	0.4	(0.1–0.9)
PFTrDA	-[a]	-[a]	-[a]	-[a]	0.7	(0.4–1)	3	(1–5)	0.3	(0.1–0.8)	1	(0.2–3)	2	(0.8–4)	0.6	(0.2–1)
PFTeDA	-[a]	-[a]	-[a]	-[a]	-[b]	-[b]	-[b]	-[b]	-[b]	-[b]	2	(0.2–5)	2	(0.9–5)	0.8	(0.2–2)
PFHxDA	-[a,b]	-[a,b]	-[a,b]	-[a,b]	-[b]	-[b]	-[b]	-[b]	-[b]	-[b]	0.3	-[c]	3	(2–4)	0.2	-[c]
PFHxS	-[b]	-[b]	0.16	(0.09–0.3)	3	(1–4)	14	(4–31)	0.3	(0.1–0.4)	6	(4–11)	4	(2–8)	1	(0.2–3)
PFOS	0.5	(0.1–1)	0.2	(0.1–0.4)	0.9	(0.4–2)	6	(2–16)	0.2	(0.1–0.3)	4	(2–7)	5	(2–12)	1	(0.4–2)

[a] The corresponding compound was not detected in the water sample.
[b] The corresponding compound was not detected in the plants.
[c] The corresponding compound was only detected once in the plants.

accumulated more in the shoots than in the roots due to the translocation produced by the water potential gradient created by plant transpiration that promotes the upward transport through the xylem. By contrast, long-chain PFASs preferentially accumulated in the roots due to the proteinphilic-linked sorption. This was also demonstrated by the TF values (Table 1), which decreased with increasing chain length, as reported in previous studies (Blaine et al., 2014; Liu et al., 2017). Bizkarguenaga et al. (2016) observed that PFOA was taken up in the translocation stream and accumulated more than PFOS in the edible part of lettuce. Krippner et al. (2014) also showed that in maize, PFBA, PFPeA, and PFHxA were more readily translocated from the roots to the shoots compared to long-chain PFASs, which bounded strongly to the surface of the roots, presumably because long-chain PFASs positively correlate with the protein content (Wen et al., 2016). However, environmental concentration and the protein and lipid contents of the plant alongside different translocation processes may explain the differences among the species. Moreover, chemical properties such as polarity, molecular size, and functional group are key in the penetration through the plasma membrane of root cells (Krippner et al., 2014). No differences in the translocation of PFASs in the roots and shoots between the two rooted species were observed.

In the Dongzhulong and Xiaoqing River area, previous studies have reported crop bioaccumulation and human exposure to PFASs (Liu et al., 2019b), suggesting that the area is contaminated at levels that can affect food safety and the environment. Because PFASs are taken up by plants, its use can be proposed as a phytoremediation procedure to eliminate the loads of these contaminants (Huff et al., 2020), as demonstrated for juncus (Zhang et al., 2019) and macrophytes (Pi et al., 2017). *L. minor* has a large proliferation rate, a high uptake capacity (Boudreau et al., 2003; Pietrini et al., 2019), and is considered a good phytoremediator of PFASs in surface water (Zhang and Liang, 2020). Similarly, *C. demersum* was previously used in PFAS bioaccumulation studies in natural environments (Babut et al., 2017; Shi et al., 2012). Regarding rooted species, *A. sessilis* was previously used in the phytoremediation of nitrate (Thurairajah and Gnanavelrajah, 2017), PCBs (Salimizadeh et al., 2020), and heavy metals (Liu et al., 2007; Wang and Qin, 2006). *E. villosa* is a widely spread pest and its uptake capacity was evaluated at a super-large antimony deposit in China (Qi et al., 2011). The target species used in the present study can be used as pollutant remediators in freshwater environments due to their uptake mechanisms (Dixit et al., 2011).

4. Conclusions

This study investigated the environmental impact of the fluoropolymer-producing facility located next to the Dongzhulong and Xiaoqing River aquatic environment, focusing on the behavior of PFASs in the water-sediment-plant system. A dilution of ∑PFASs was observed along the river in all the matrices. According to the PCA, PFOA was the main contaminant in the water and sediments due to the point source contamination from the Gongyue Group facility, while PFSAs were punctually detected and attributed to urban discharges. K_d values indicated that long-chain PFASs preferentially remained sorbed in the sediment, while short-chain PFASs were mobile in the water column and taken up by different plant species. Differences between the floating and rooted plants were observed, with floating species easily taking up long-chain PFASs directly from the water and rooted species competing with the sediment for the uptake of PFASs. Moreover, in the rooted species, long-chain PFASs remained accumulated in the roots because of protein affinity, while short-chain PFASs were more mobile and translocated to the shoots. Overall, this study provides new information on the occurrence and distribution of PFASs in a river basin, sediment accumulation, and plant uptake in real environmental conditions, which is useful in assessing the final fate of PFASs in areas highly affected by direct discharges and environmental pollution.

CRediT authorship contribution statement

Pere Colomer-Vidal: Conceptualization, Investigation, Formal analysis, Writing – original draft, Writing – review & editing. **Longfei Jiang:** Conceptualization, Investigation, Writing – review & editing. **Weiping Mei:** Conceptualization, Investigation, Writing – review & editing. **Chunling Luo:** Conceptualization, Investigation, Validation, Writing – review & editing, Supervision, Project administration, Funding acquisition. **Silvia Lacorte:** Conceptualization, Investigation, Validation, Writing – review & editing, Supervision, Funding acquisition. **Anna Rigol:** Conceptualization, Investigation, Validation, Writing – review & editing, Supervision. **Gan Zhang:** Supervision, Project administration, Funding acquisition.

Declaration of Competing Interest

The authors declare that they have no known competing financial interests or personal relationships that could have appeared to influence the work reported in this paper.

Acknowledgments

Pere Colomer Vidal acknowledges the funding from the European Union Europe Aid 'SEW-REAP' project [ECRIP ICI+/2014/348–010]. The Spanish Ministry of Science and Innovation under the grant PID2019–105732GB-C21 and the Local Innovative and Research Teams Project of the Guangdong Pearl River Talents Program (2017BT01Z134) provided financial support. Dr. Chunling Luo would like to thank the support from the Ten Thousand Talent Program of the Organization Department of the Central Committee of the CPC.

This work was carried out at the facilities of the Guangzhou Institute of Geochemistry.

Appendix A. Supporting information

Supplementary data associated with this article can be found in the online version at doi:10.1016/j.jhazmat.2021.126768.

References

Babut, M., Labadie, P., Simonnet-Laprade, C., Munoz, G., Roger, M.C., Ferrari, B.J.D., Budzinski, H., Sivade, E., 2017. Per- and poly-fluoroalkyl compounds in freshwater fish from the Rhône River: influence of fish size, diet, prey contamination and biotransformation. Sci. Total Environ. 605–606, 38–47. https://doi.org/10.1016/j.scitotenv.2017.06.111.

Barton, K.E., Starling, A.P., Higgins, C.P., McDonough, C.A., Calafat, A.M., Adgate, J.L., 2020. Sociodemographic and behavioral determinants of serum concentrations of per- and polyfluoroalkyl substances in a community highly exposed to aqueous film-forming foam contaminants in drinking water. Int. J. Hyg. Environ. Health 223, 256–266. https://doi.org/10.1016/j.ijheh.2019.07.012.

Bizkarguenaga, E., Zabaleta, I., Mijangos, L., Iparraguirre, A., Fernández, L.A., Prieto, A., Zuloaga, O., 2016. Uptake of perfluorooctanoic acid, perfluorooctane sulfonate and perfluorooctane sulfonamide by carrot and lettuce from compost amended soil. Sci. Total Environ. 571, 444–451. https://doi.org/10.1016/j.scitotenv.2016.07.010.

Blaine, A.C., Rich, C.D., Sedlacko, E.M., Hyland, K.C., Stushnoff, C., Dickenson, E.R.V., Higgins, C.P., 2014. Perfluoroalkyl acid uptake in lettuce (*Lactuca sativa*) and Strawberry (*Fragaria ananassa*) irrigated with reclaimed water. Environ. Sci. Technol. 48, 14361–14368. https://doi.org/10.1021/es504150h.

Boudreau, T.M., Sibley, P.K., Mabury, S.A., Muir, D.G.C., Solomon, K.R., 2003. Laboratory evaluation of the toxicity of perfluorooctane sulfonate (PFOS) on *Selenastrum capricornutum*, *Chlorella vulgaris*, *Lemna gibba*, *Daphnia magna*, and *Daphnia pulicaria*. Arch. Environ. Contam. Toxicol. 44, 307–313. https://doi.org/10.1007/s00244-002-2102-6.

Buck, R.C., Franklin, J., Berger, U., Conder, J.M., Cousins, I.T., Voogt, P., De, Jensen, A. A., Kannan, K., Mabury, S.A., van Leeuwen, S.P.J., 2011. Perfluoroalkyl and polyfluoroalkyl substances in the environment: terminology, classification, and origins. Integr. Environ. Assess. Manag. 7, 513–541. https://doi.org/10.1002/ieam.258.

Chen, H., Sun, R., Zhang, C., Han, J., Wang, X., Han, G., He, X., 2016. Occurrence, spatial and temporal distributions of perfluoroalkyl substances in wastewater, seawater and sediment from Bohai Sea. China Environ. Pollut. 219, 389–398. https://doi.org/10.1016/j.envpol.2016.05.017.

Chen, H., Wang, X., Zhang, C., Sun, R., Han, J., Han, G., Yang, W., He, X., 2017. Occurrence and inputs of perfluoroalkyl substances (PFASs) from rivers and drain

outlets to the Bohai Sea, China. Environ. Pollut. 221, 234–243. https://doi.org/10.1016/j.envpol.2016.11.070.
Cousins, I.T., Goldenman, G., Herzke, D., Lohmann, R., Miller, M., Ng, C.A., Patton, S., Scheringer, M., Trier, X., Vierke, L., Wang, Z., DeWitt, J.C., 2019. The concept of essential use for determining when uses of PFASs can be phased out. Environ. Sci. Process. Impacts 21, 1803–1815. https://doi.org/10.1039/C9EM00163H.
Dixit, A., Dixit, S., Goswami, C., 2011. Process and plants for wastewater remediation: a review. Sci. Rev. Chem. Commun. 1, 71–77.
Ghisi, R., Vamerali, T., Manzetti, S., 2019. Accumulation of perfluorinated alkyl substances (PFAS) in agricultural plants: a review. Environ. Res. 169, 326–341. https://doi.org/10.1016/j.envres.2018.10.023.
Gorrochategui, E., Lacorte, S., Tauler, R., Martin, F.L., 2016. Perfluoroalkylated substance effects in *Xenopus laevis* A6 kidney epithelial cells determined by ATR-FTIR spectroscopy and chemometric analysis. Chem. Res. Toxicol. 29, 924–932. https://doi.org/10.1021/acs.chemrestox.6b00076.
Heydebreck, F., Tang, J., Xie, Z., Ebinghaus, R., 2015. Alternative and legacy perfluoroalkyl substances: differences between european and Chinese river/estuary systems. Environ. Sci. Technol. 49, 8386–8395. https://doi.org/10.1021/acs.est.5b01648.
Higgins, C.P., Luthy, R.G., 2006. Sorption of perfluorinated surfactants on sediments. Environ. Sci. Technol. 40, 7251–7256. https://doi.org/10.1021/es061000n.
Huff, D.K., Morris, L.A., Sutter, L., Costanza, J., Pennell, K.D., 2020. Accumulation of six PFAS compounds by woody and herbaceous plants: potential for phytoextraction. Int. J. Phytoremediat. 0, 1–13. https://doi.org/10.1080/15226514.2020.1786004.
Krippner, J., Brunn, H., Falk, S., Georgii, S., Schubert, S., Stahl, T., 2014. Effects of chain length and pH on the uptake and distribution of perfluoroalkyl substances in maize (*Zea mays*). Chemosphere 94, 85–90. https://doi.org/10.1016/j.chemosphere.2013.09.018.
Liu, J., Dong, Y., Xu, H., Wang, D., Xu, J., 2007. Accumulation of Cd, Pb and Zn by 19 wetland plant species in constructed wetland. J. Hazard. Mater. 147, 947–953. https://doi.org/10.1016/j.jhazmat.2007.01.125.
Liu, Y., Zhang, Y., Li, J., Wu, N., Li, W., Niu, Z., 2019a. Distribution, partitioning behavior and positive matrix factorization- based source analysis of legacy and emerging polyfluorinated alkyl substances in the dissolved phase, surface sediment and suspended particulate matter around coastal areas of Boha. Environ. Pollut. 246, 34–44. https://doi.org/10.1016/j.envpol.2018.11.113.
Liu, Z., Lu, Y., Shi, Y., Wang, P., Jones, K., Sweetman, A.J., Johnson, A.C., Zhang, M., Zhou, Y., Lu, X., Su, C., Sarvajayakesavaluc, S., Khan, K., 2017. Crop bioaccumulation and human exposure of perfluoroalkyl acids through multi-media transport from a mega fluorochemical industrial park, China. Environ. Int. 106, 37–47. https://doi.org/10.1016/j.envint.2017.05.014.
Liu, Z., Lu, Y., Song, X., Jones, K., Sweetman, A.J., Johnson, A.C., Zhang, M., Lu, X., Su, C., 2019b. Multiple crop bioaccumulation and human exposure of perfluoroalkyl substances around a mega fluorochemical industrial park, China: implication for planting optimization and food safety. Environ. Int. 127, 671–684. https://doi.org/10.1016/j.envint.2019.04.008.
Mhadhbi, L., Rial, D., Pérez, S., Beiras, R., 2012. Ecological risk assessment of perfluorooctanoic acid (PFOA) and perfluorooctanesulfonic acid (PFOS) in marine environment using *Isochrysis galbana*, *Paracentrotus lividus*, *Siriella armata* and *Psetta maxima*. J. Environ. Monit. 14, 1375–1382. https://doi.org/10.1039/c2em30037k.
Milinovic, J., Lacorte, S., Vidal, M., Rigol, A., 2015. Sorption behaviour of perfluoroalkyl substances in soils. Sci. Total Environ. 511, 63–71. https://doi.org/10.1016/j.scitotenv.2014.12.017.
Oliaei, F., Kriens, D., Weber, R., Watson, A., 2013. PFOS and PFC releases and associated pollution from a PFC production plant in Minnesota (USA). Environ. Sci. Pollut. Res. 20, 1977–1992. https://doi.org/10.1007/s11356-012-1275-4.
Pi, N., Ng, J.Z., Kelly, B.C., 2017. Uptake and elimination kinetics of perfluoroalkyl substances in submerged and free-floating aquatic macrophytes: results of mesocosm experiments with *Echinodorus horemanii* and *Eichhornia crassipes*. Water Res. 117, 167–174. https://doi.org/10.1016/j.watres.2017.04.003.
Pietrini, F., Passatore, L., Fischetti, E., Carloni, S., Ferrario, C., Polesello, S., Zacchini, M., 2019. Evaluation of morpho-physiological traits and contaminant accumulation ability in *Lemna minor* L. treated with increasing perfluorooctanoic acid (PFOA) concentrations under laboratory conditions. Sci. Total Environ. 695, 133828 https://doi.org/10.1016/j.scitotenv.2019.133828.
Qi, C., Wu, F., Deng, Q., Liu, G., Mo, C., Liu, B., Zhu, J., 2011. Distribution and accumulation of antimony in plants in the super-large Sb deposit areas, China. Microchem. J. 97, 44–51. https://doi.org/10.1016/j.microc.2010.05.016.
Renner, R., 2006. Sorting out sources of perfluorinated chemicals. Environ. Sci. Technol. 40, 2866–2867.
Renner, R., 2001. Growing concern over perfluorinated chemicals. Environ. Sci. Technol. 35, 154A–160A. https://doi.org/10.1021/es012317k.
Salimizadeh, M., Shirvani, M., Shariatmadari, H., Mortazavi, M.S., 2020. Bentonite addition to a PCB-contaminated sandy soil improved the growth and phytoremediation efficiency of *Zea mays* L. and *Alternanthera sessilis* L. Int. J. Phytoremediat. 22, 176–183. https://doi.org/10.1080/15226514.2019.1652564.
Shi, Y., Pan, Y., Wang, J., Cai, Y., 2012. Distribution of perfluorinated compounds in water, sediment, biota and floating plants in Baiyangdian Lake, China. J. Environ. Monit. 14, 636–642. https://doi.org/10.1039/C1EM10772K.
Shi, Y., Vestergren, R., Xu, L., Song, X., Niu, X., Zhang, C., Cai, Y., 2015. Characterizing direct emissions of perfluoroalkyl substances from ongoing fluoropolymer production sources: a spatial trend study of Xiaoqing River, China. Environ. Pollut. 206, 104–112. https://doi.org/10.1016/j.envpol.2015.06.035.
Song, X., Vestergren, R., Shi, Y., Huang, J., Cai, Y., 2018. Emissions, transport, and fate of emerging per- and polyfluoroalkyl substances from one of the major fluoropolymer manufacturing facilities in China. Environ. Sci. Technol. 52, 9694–9703. https://doi.org/10.1021/acs.est.7b06657.
Sonne, C., Siebert, U., Gonnsen, K., Desforges, J.P., Eulaers, I., Persson, S., Roos, A., Bäcklin, B.M., Kauhala, K., Tange Olsen, M., Harding, K.C., Treu, G., Galatius, A., Andersen-Ranberg, E., Gross, S., Lakemeyer, J., Lehnert, K., Lam, S.S., Peng, W., Dietz, R., 2020. Health effects from contaminant exposure in Baltic Sea birds and marine mammals: a review. Environ. Int. 139, 105725 https://doi.org/10.1016/j.envint.2020.105725.
Stahl, T., Gassmann, M., Falk, S., Brunn, H., 2018. Concentrations and distribution patterns of perfluoroalkyl acids in sewage sludge and in biowaste in Hesse, Germany. J. Agric. Food Chem. 66, 10147–10153. https://doi.org/10.1021/acs.jafc.8b03063.
Tabachnick, B.G., Fidell, L.S., 2000. Computer-Assisted Research Design and Analysis, 1st ed. Allyn & Bacon, Inc, USA.
Thurairajah, S., Gnanavelrajah, N., 2017. Ipomoea aquatica and Alternanthera sessilis to remediate ground water contaminated with nitrate. "Greener Agric. Environ. through Converg. Technol. Proc. Int. Symp. Agric. Environ. - ISAE 2017, 19th January 2017, Univ. Ruhuna, Sri Lanka.
Wang, W., Rhodes, G., Ge, J., Yu, X., Li, H., 2020. Uptake and accumulation of per- and polyfluoroalkyl substances in plants. Chemosphere 261, 127584. https://doi.org/10.1016/j.chemosphere.2020.127584.
Wang, P., Lu, Y., Wang, T., Fu, Y., Zhu, Z., Liu, S., Xie, S., Xiao, Y., Giesy, J.P., 2014c. Occurrence and transport of 17 perfluoroalkyl acids in 12 coastal rivers in south Bohai coastal region of China with concentrated fluoropolymer facilities. Environ. Pollut. 190, 115–122. https://doi.org/10.1016/j.envpol.2014.03.030.
Wang, X.S., Qin, Y., 2006. Removal of Ni(II), Zn(II) and Cr(VI) from aqueous solution by Alternanthera philoxeroides biomass. J. Hazard. Mater. 138, 582–588. https://doi.org/10.1016/j.jhazmat.2006.05.091.
Wang, Z., Cousins, I.T., Scheringer, M., Buck, R.C., Hungerbühler, K., 2014a. Global emission inventories for C4-C14 perfluoroalkyl carboxylic acid (PFCA) homologues from 1951 to 2030, Part I: Production and emissions from quantifiable sources. Environ. Int. 70, 62–75. https://doi.org/10.1016/j.envint.2014.04.013.
Wang, Z., Cousins, I.T., Scheringer, M., Buck, R.C., Hungerbühler, K., 2014b. Global emission inventories for C4-C14 perfluoroalkyl carboxylic acid (PFCA) homologues from 1951 to 2030, part II: The remaining pieces of the puzzle. Environ. Int. 69, 166–176. https://doi.org/10.1016/j.envint.2014.04.006.
Wen, B., Li, L., Liu, Y., Zhang, H., Hu, X., Shan, X. quan, Zhang, S., 2013. Mechanistic studies of perfluorooctane sulfonate, perfluorooctanoic acid uptake by maize (*Zea mays* L. cv. TY2). Plant Soil 370, 345–354. https://doi.org/10.1007/s11104-013-1637-9.
Wen, B., Wu, Y., Zhang, H., Liu, Y., Hu, X., Huang, H., Zhang, S., 2016. The roles of protein and lipid in the accumulation and distribution of perfluorooctane sulfonate (PFOS) and perfluorooctanoate (PFOA) in plants grown in biosolids-amended soils. Environ. Pollut. 216, 682–688. https://doi.org/10.1016/j.envpol.2016.06.032.
Xie, S., Wang, T., Liu, S., Jones, K.C., Sweetman, A.J., Lu, Y., 2013. Industrial source identification and emission estimation of perfluorooctane sulfonate in China. Environ. Int. 52, 1–8. https://doi.org/10.1016/j.envint.2012.11.004.
Zhang, W., Liang, Y., 2020. Removal of eight perfluoroalkyl acids from aqueous solutions by aeration and duckweed. Sci. Total Environ. 724, 138357 https://doi.org/10.1016/j.scitotenv.2020.138357.
Zhang, W., Zhang, D., Zagorevski, D.V., Liang, Y., 2019. Exposure of Juncus effusus to seven perfluoroalkyl acids: uptake, accumulation and phytotoxicity. Chemosphere 233, 300–308. https://doi.org/10.1016/j.chemosphere.2019.05.258.
Zhang, Y., Meng, W., Guo, C., Xu, J., Yu, T., Fan, W., Li, L., 2012. Determination and partitioning behavior of perfluoroalkyl carboxylic acids and perfluorooctanesulfonate in water and sediment from Dianchi Lake, China. Chemosphere 88, 1292–1299. https://doi.org/10.1016/j.chemosphere.2012.03.103.
Zhao, Z., Tang, J., Mi, L., Tian, C., Zhong, G., Zhang, G., Wang, S., Li, Q., Ebinghaus, R., Xie, Z., Sun, H., 2017. Perfluoroalkyl and polyfluoroalkyl substances in the lower atmosphere and surface waters of the Chinese Bohai Sea, Yellow Sea, and Yangtze River estuary. Sci. Total Environ. 599–600, 114–123. https://doi.org/10.1016/j.scitotenv.2017.04.147.
Zhao, Z., Tang, J., Xie, Z., Chen, Y., Pan, X., Zhong, G., Sturm, R., Zhang, G., Ebinghaus, R., 2013. Perfluoroalkyl acids (PFAAs) in riverine and coastal sediments of Laizhou Bay, North China. Sci. Total Environ. 447, 415–423. https://doi.org/10.1016/j.scitotenv.2012.12.095.
Zhou, Y., Wang, T., Li, Q., Wang, P., Li, L., Chen, S., Zhang, Y., Khan, K., Meng, J., 2018. Spatial and vertical variations of perfluoroalkyl acids (PFAAs) in the Bohai and Yellow Seas: bridging the gap between riverine sources and marine sinks. Environ. Pollut. 238, 111–120. https://doi.org/10.1016/j.envpol.2018.03.027.
Zhu, Z., Wang, T., Wang, P., Lu, Y., Giesy, J.P., 2014. Perfluoroalkyl and polyfluoroalkyl substances in sediments from South Bohai coastal watersheds, China. Mar. Pollut. Bull. 85, 619–627. https://doi.org/10.1016/j.marpolbul.2013.12.042.